# Late Cretaceous subsidence in Wyoming: Quantifying the dynamic component

Shaofeng Liu Faculty of Geosciences and Resources, China University of Geosciences, Beijing 100083, China, and Institute for Energy Research, Department of Geology and Geophysics, University of Wyoming, Laramie, Wyoming 82071, USA

Dag Nummedal Institute for Energy Research, Department of Geology and Geophysics, University of Wyoming, Laramie, Wyoming 82071, USA

## ABSTRACT

**The Late Cretaceous Western Interior Basin of North America is generally considered to have been a retroarc foreland basin. Flexural backstripping of the stratigraphic record from 97.2 Ma to 73.4 Ma, along a section perpendicular to the Wyoming-Idaho salient of the Sevier belt, clearly demonstrates that there were components of subsidence in addition to those driven by the thrust and associated sediment loads. The simulation demonstrates that the flexural foredeep is only ~180–120 km wide and shows a forebulge located near the subsequent Laramide Rock Springs uplift. Foredeep strata between the Rock Springs uplift on the east and the thrust front to the west were mostly involved in the eastward-overlapping thrust belt or deeply truncated by inferred rebound after 78.5 Ma. The difference between the observed, decompacted, cumulative subsidence and the amount of subsidence that can be explained by simple flexural loading, the "residual" subsidence, increases from ~800 m in eastern Wyoming to ~1.8 km near the thrust belt. The westward-thickening Upper Cretaceous sediment wedge filled the accommodation space generated by downward tilting to the west of the North American cratonic margin by underplating and mantle flow associated with the shallowly subducted Farallon plate.**

**Keywords:** subsidence, simulation, dynamic component, foreland basin, Wyoming.

## INTRODUCTION

The Cretaceous Western Interior Basin is generally thought of as a foreland basin because of the asymmetric westward-thickening sediment wedge (Cross, 1986) and its relationship to the Sevier thrust belt along its western margin (Royse, 1993; DeCelles, 1994). A flexural study by Jordan (1981) demonstrated that the subsidence and sedimentation that characterized the Cretaceous Western Interior Basin were shaped by loading of the Sevier thrust belt and loading of the sediment fill of the foreland basin. Jordan (1981) identified 600 m "excess sediment thickness" relative to the flexed foreland basin. That difference was attributed to sea-level rise in the Late Cretaceous. However, the global long-term change in the Late Cretaceous was sea-level fall (Abreu et al., 1998). Therefore, the excess accommodation space identified by Jordan (1981) implies the presence of a regional tectonic-subsidence component, not global sea-level change. Cross (1986) inferred that subsidence of the basin from before ca. 92 to 82 Ma was confined to a relatively narrow zone east of the Sevier belt and was due to lithospheric flexure induced by loading of thrust plates and sedimentary deposits. In contrast, subsidence from ca. 80 to 67 Ma, which occurred over a broad region centered about Colorado and Wyoming, was due to sublithospheric loading and cooling induced by the shallowly subducted oceanic (Farallon) plate. Two-dimensional flexural backstripping by Pang and Nummedal (1995) demonstrated that the flexural subsidence recorded in Cenomanian to lower Campanian strata (97–80 Ma) resulted from thrust loading superimposed on dynamic background subsidence.

Consensus appears to have been reached that the Western Interior Basin was a combined product of thrusting in the Sevier belt, sedimentary filling of the basin, and regional dynamic loads. However, a quantitative differentiation of the loads has not yet been carried out. This paper addresses that issue by using a new basin cross section extending ~500 km east from the thrust front and constructed from detailed well-log correlations of Upper Cretaceous rocks. The calculations are based on the latest $^{40}Ar/^{39}Ar$–derived Late Cretaceous time scale (Obradovich, 1993) and on loads determined from a cross section traversing the Sevier thrust belt (Royse, 1993) in which the deformation, shortening, and erosion were restored. The difference between the total observed, decompacted subsidence and that due to the surface load is inferred to be a result of dynamic subsidence. This study is the first published attempt to actually quantify the magnitude of the dynamic component of subsidence. Moreover, the precision that we achieve on the magnitude of the subsidence, its timing, and its wavelength provides the first accurate constraints on dynamic models of mantle flow.

## METHODOLOGY

### Reconstructing and Decompacting the Sediment Fill

Upper Cretaceous strata of the U.S. Western Interior Basin are well suited for flexural analysis because of precise stratigraphic constraints (Gill and Cobban, 1973; Kauffman et al., 1993; Obradovich, 1993). The modeled section crosses southern Wyoming from the Idaho-Wyoming thrust-belt salient, across the Moxa arch and the Greater Green River, Laramie, and Cheyenne Basins (Fig. 1). The modeled succession spans the Cenomanian to Campanian Stages. Figure 2 is the result of well-log correlations along this cross section.

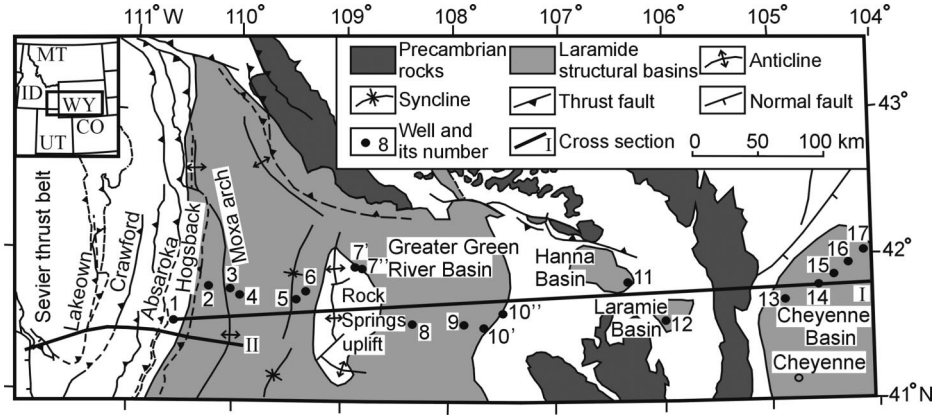


**Figure 1. Idaho-Wyoming salient of Sevier thrust belt and its associated basins across southern Wyoming, showing locations of cross sections I and II (Figs. 2 and 3). MT, Montana; ID, Idaho; WY, Wyoming; CO, Colorado; UT, Utah.**

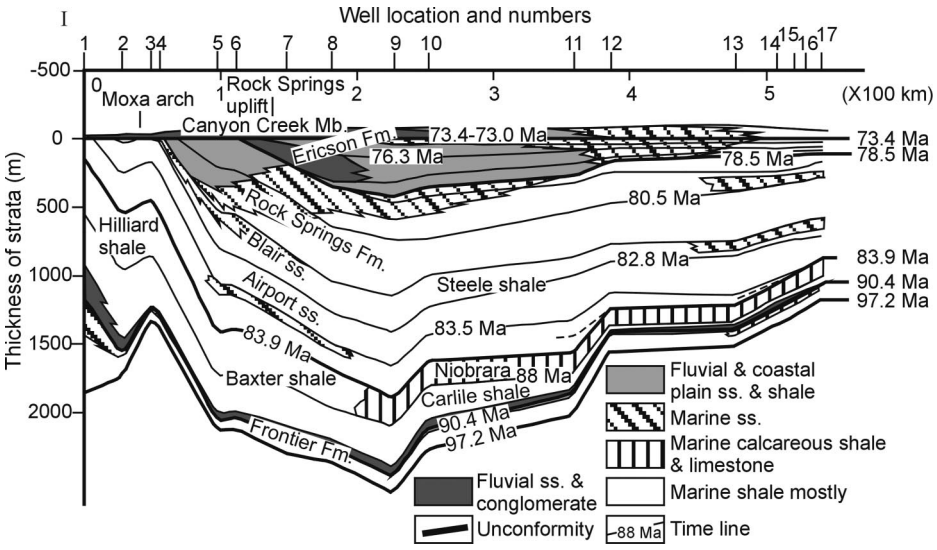


**Figure 2. Results of correlation of 19 well logs along cross section I (Fig. 1), covering stratigraphic interval from middle Cenomanian base of Frontier Formation to upper Campanian Ericson Formation. Wells 7 and 10 include two logs sampling different intervals (well 7′ and 7″ and well 10′ and 10″ in Fig. 1) in order to get complete stratigraphic columns. This is section I in Figure 1; Fm, Formation; Mb, Member; ss, sandstone.**

The cross section is new, yet we were aided considerably in its construction by the previous work of Dyman et al. (1994). The formations included are the Frontier Formation, Baxter shale, Blair Formation, Rock Springs Formation, Ericson Formation (lower part), and their correlatives. Time-stratigraphic correlations were based on the physical continuity of time-parallel marker beds, such as limestone tops, bentonite beds, unconformities, and shale beds, all of which generate distinctive and traceable log patterns (Merewether et al., 1984).

We chose five reference levels, corresponding to the ages of 97.2, 90.4, 83.9, 78.5, and 73.4 Ma (Fig. 2), and successively removed overlying strata in the analysis. The decompacted sediment thicknesses and their average densities were used as components of the input loads in the flexural modeling.

## Restoring Original Thrust Load

Thrust-load estimates are derived from cross section GG′ of Royse (1993; section II in Fig. 1) that traverses the Sevier thrust belt immediately west of the end of our restored basin-wide stratigraphic cross section (section I in Fig. 1). Four main thrusts are arranged in an eastward overlapping array in the section (Fig. 3). The timing of deformation in the Sevier thrust belt was as follows (see Coogan and Royse, 1990; Royse, 1993; DeCelles, 1994; Yonkee et al., 1997): (1) the Meade-Laketown thrusting occurred from the middle Cenomanian through late Turonian (ca. 97.2–90.4 Ma); (2) the Crawford thrusting occurred from the late Turonian through the Santonian (ca. 90.4–83.9 Ma); (3) the ‘‘early Absaroka’’ thrusting lasted from the end of the Santonian through the early Campanian (ca. 83.9–78.5 Ma); and the ‘‘quiescence phase’’ was from the early to late Campanian (ca. 78.5–73.4 Ma), prior to the onset of late Absaroka thrusting and early Paleocene movement on the Hogsback thrust.

A series of sequentially restored cross sections across the thrust belt ca. 90.4, 83.9, 78.5, and 73.4 Ma was reconstructed by setting the eastern end of the section as a reference point. The deformation and shortening of the Hogsback, Absaroka, and Crawford faults were restored and balanced (Fig. 3). All published information was utilized to constrain the stratigraphic distribution and thrust-belt thickness (data from Royse [1993] and DeCelles [1994]). The strata that were exposed in the thrust belt at different stages were determined by the pebble composition of the basin deposits, and the mountain profiles were constructed by thrust faults and deformed strata. We assumed that the restored strata had thicknesses equal to their preserved parts. The final sequentially restored cross sections represent the whole thrust load and restored basin deposits involved in the thrust deformation at four reference times. Restoration indicates that the thrust belt reached a maximum elevation of 4.8 km at the location of the present-day Wasatch Range. Model analysis indicates that the thrust-belt elevation is isostatically compensated.

In light of the uncertainty about section restorations and load distribution, we performed sensitivity analyses by performing simulations for different geometries on the basement-involved Crawford thrust, for different maximum elevations of the Sevier thrust belt, and for different manifestations of the hinterland load to the west of the Wasatch culmination. The resulting model changes in the dynamic subsidence profile are negligible (<1%).

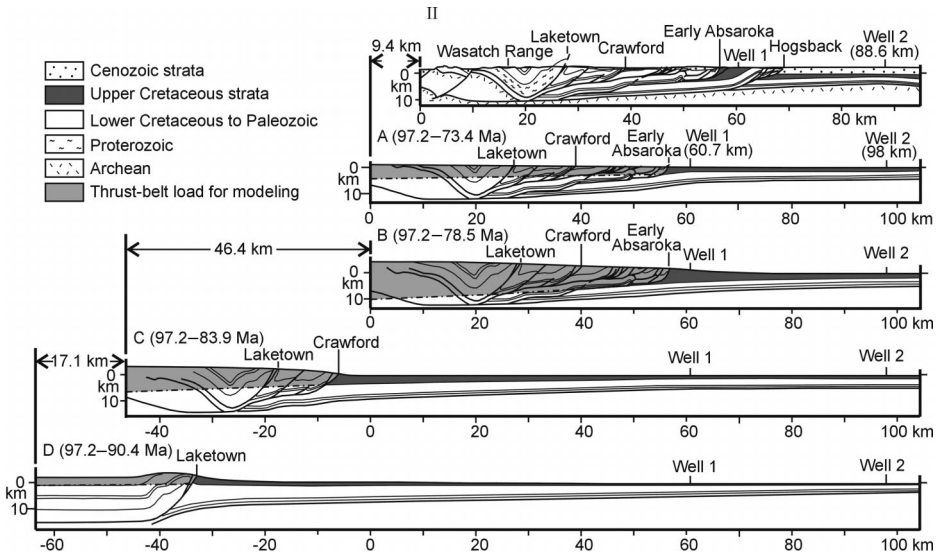


**Figure 3. Sequential restoration of Sevier thrust belt, based on cross section GG′ of Royse (1993). Deformation and shortening of Hogsback, Absaroka, and Crawford faults were balanced, mountain profiles restored, and deformed basin fill rebuilt. This is section II in Figure 1.**

### Flexural Backstripping

Flexural-backstripping methodology is similar to that used by Jordan (1981), and Flemings and Jordan (1990), and is not discussed further here. The backstripping was conducted in two steps. First, we used only the thrust load to forward model the foredeep and the forebulge; then the load of the sediment wedge was added to the simulation to reconstruct the complete basin shape. Finally, the simulated subsidence for the combined thrust

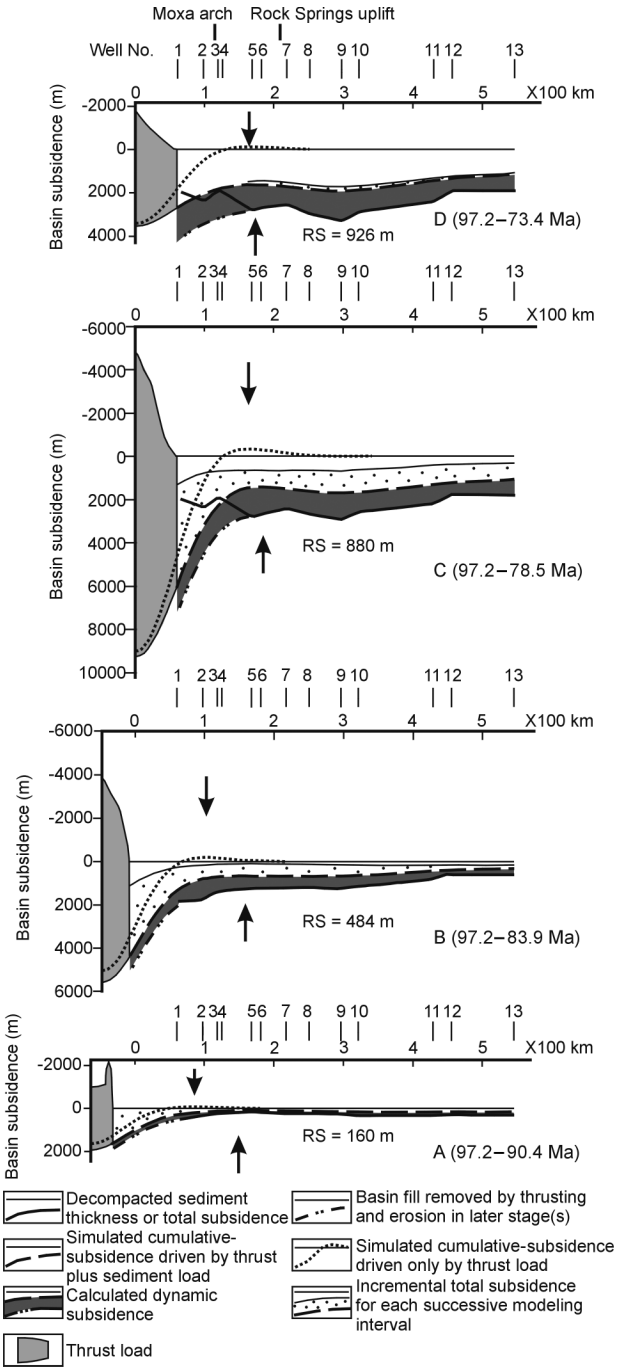


**Figure 4. Flexurally backstripped subsidence profiles across thrust belt and basin over four cumulative time intervals. Upper and lower arrows track movement of forebulge in response to load of only thrust belt and load of thrust belt plus sediments, respectively. Flexural rigidity used for this calculation was $10^{22.5}$ N·m. RS—residual subsidence; numbers indicate wells located in Figure 1.**

and sediment loads was subtracted from the total, decompacted subsidence to calculate the residual.

## RESULTS

Computed subsidence profiles for the elastic lithosphere along the cross section in Figure 1, for the time intervals of 97.2–90.4 Ma, 97.2–83.9 Ma, 97.2–78.5 Ma, and 97.2–73.4 Ma, are presented in Figure 4. A range of flexural rigidities, $10^{21}$, $10^{22}$, $10^{22.5}$, $10^{23}$, and $10^{24}$ N·m, was analyzed in this modeling, and $10^{22.5}$ N·m provided consistently the best fit in which predicted and observed subsidence profiles were parallel at all different stages.

Simulation of crustal loading by only the thrust belt (shown in light shading at the left side of each profile in Fig. 4) produces asymmetrical cumulative-subsidence curves (dotted lines in Fig. 4), which represent a foredeep and a forebulge that rises above the zero level. The simulation documents progressive eastward forebulge migration (upper arrows). During the period of tectonic quiescence between the early and late Absaroka thrusts (78.5–73.4 Ma), the forebulge stopped migrating and decreased in amplitude, and the foredeep rebounded dramatically (Figs. 4C and 4D). To the east of the forebulge there is no detectable basin subsidence caused by thrust loading.

The next modeling step included the two components of sediment load. One is the preserved sediment shown above the heavy solid lines in Figure 4; the other is the restored sediment wedge near the thrust belt that has been removed by subsequent thrusting and erosion, the thickness of which was assumed to fit the adjacent preserved sediment thickness and also conform to the shape of the total subsidence curve. This restored sediment thickness is shown by a dashed line with two dots in Figure 4. At any given time of thrusting, this sediment load was on the basinward side of the leading thrust. The simulated cumulative subsidence curves (heavy dashed lines in Fig. 4) caused by the whole thrust load plus the original sediment load in general parallel the observed total subsidence curves (heavy solid lines). The simulation shows a narrow foredeep (~180–120 km wide) and a very gentle forebulge in front of the thrust belt. The forebulge migration in response to this complete load shows a slightly different pattern (lower arrows in Fig. 4). It is lower in amplitude than the one predicted by the thrust-belt load alone, and the simulated forebulges migrate eastward in the first three time steps and move back toward the west in the final step (Fig. 4). The residual subsidence—the difference between the final simulated cumulative subsidence and the observed total subsidence (dark gray band in Fig. 4)—develops a westward-thickening wedge, and its average thickness gradually increases from ~160 m in the first stage, to 484 m in the second stage, to 880 m in the third stage, and to 926 m at the last stage. The results of the calculated incremental subsidence for each of the four time intervals are shown as dot-patterned bands in Figure 4. The foredeep strata deposited to the west of the ~180 km mark in the first three time steps of the modeling were mostly eroded or incorporated in the thrust belt in later stages. During the fourth modeling step (Figs. 4C to Fig. 4D), the thrust belt and foredeep rebounded isostatically because of erosion during the tectonically quiescent phase. The balance between the rate of isostatic rebound and residual subsidence controlled the generation of local accommodation space above this unconformity, into which space the basal Ericson Formation was deposited. The observed westward basal onlap of the lower Ericson (upper left of Fig. 2) is consistent with a gradual decrease in the isostatic rebound and a shift to control of local sediment accommodation by residual subsidence.

## DISCUSSION

The results demonstrate that sediment accommodation and erosion in Wyoming in the Late Cretaceous were controlled by flexural loading during thrusting in the Sevier orogenic belt, isostatic rebound during tectonic quiescence, and a dynamic component of subsi-

dence. Flexural subsidence during the modeled time interval reached a maximum of ~6 km near the thrust belt in the earliest Campanian (at 78.5 Ma), rebounding by ~3 km at the end of the tectonically quiet phase (at 73.4 Ma). The wavelength of this subsidence is the width of the foredeep, ~180–120 km. When the load of the sediment wedge is added to that of the thrust belt, we also find that the forebulge is reduced to only a region of lesser subsidence; it never rises above the ''zero level.''

Total subsidence during the modeled interval exceeded that due to flexure by ~1 km and a wavelength that exceeds the width of the studied profile (600 km). We infer that the Late Cretaceous accommodation space documented by Bunker et al. (1988) across Nebraska and Iowa records this same background subsidence; its wavelength, therefore, exceeds 1500 km. Because the wavelength of subsidence is proportional to the thickness of the deforming substrate, processes involving the mantle caused the background subsidence documented in this study. We think it records the dynamic topography generated by eastward subduction of the Farallon plate beneath North America (Burgess et al., 1997).

The findings are consistent with theoretical modeling by Gurnis (1992) and Burgess et al. (1997) and with an earlier study of the entire Rocky Mountains by Pang and Nummedal (1995). Several models for dynamic subsidence due to mantle flow (e.g., Lithgow-Bertelloni and Gurnis, 1997), however, predict amplitudes greater than those observed, probably because of uncertainties related to the mantle-viscosity profile used in such models. Such is also the case for the Late Cretaceous of Wyoming, where the cumulative dynamic subsidence between 97 Ma and 73 Ma ranged from ~800 m at the eastern state line to ~1800 m near the thrust belt. In contrast, the model results of Burgess et al. (1997, their Fig. 10) imply a dynamic subsidence of 2600 m at the cratonic margin in central Utah. Given the spatial resolution of their model, as well as the extent of the subducted Farallon slab, model subsidence in western Wyoming would be about the same. The difference is well above the range of error in the calculations, and probably reflects the use of an inappropriate vertical mantle-viscosity profile. Quantification of dynamic subsidence from backstripped stratigraphic data, as done in this paper, might help improve the current global model for the mantle-viscosity structure.

## CONCLUSIONS

A well-constrained cross section of Upper Cretaceous strata across southern Wyoming was used as the basis for quantitative differentiation of subsidence mechanisms for this large retroarc basin during the interval from 97.2 to 73.4 Ma. As postulated before, the subsidence pattern is consistent with the change in subduction of the Farallon plate from steep to shallow. Accommodation for the westward-thickening wedge of sediments on this cratonic margin was provided by combined flexural loads and dynamic subsidence due to mantle flow. The associated basin was at least 1500 km wide, of which only the westernmost 180–120 km represent a flexural foreland basin. Almost all of the foredeep deposits in western Wyoming were subsequently incorporated in the Sevier thrust belt or eroded.

The effects of the two phases of Absaroka thrusting are quite evident within this foreland basin. Movement on the thrust created a foredeep that attained a maximum depth of 6 km at 78.5 Ma (early Campanian). Subsequent cessation of thrusting was associated with major foredeep rebound, creating a significant unconformity followed by deposition of the Ericson Formation as a westward-onlapping wedge (Fig. 2) of nonmarine clastic sediments.

The numerical model of Burgess et al. (1997) for dynamic topography at the western margin of the North American craton is consistent with our quantification of the dynamic subsidence component for the Late Cretaceous, except that their magnitudes for subsidence exceed our calculations by ~45%.


## ACKNOWLEDGMENTS

Funded by the Chinese Natural Science Foundation (grants 40272055, 40234041, 49732080, and 49772119), the Chinese 973 project (grant G1999043303), the Institute for Energy Research (University of Wyoming), and the Project Sponsored by the Scientific Research Foundation for the Returned Overseas Chinese Scholars, State Education Ministry (grant to Liu). We thank Paul Heller, Ronald Steel, Peigui Yin, Hongjun Luo, and Huaiyu Yuan for their help, and the Wyoming Geological Survey for providing well-log data. Peter DeCelles and Michael Gurnis provided helpful reviews of the paper.


## REFERENCES CITED


Abreu, V.S., Hardenbol, J., Haddad, G.A., Baum, G.R., Droxler, A.W., and Vail, P.R., 1998, Oxygen isotope synthesis: A Cretaceous ice-house?, *in* de Graciansky, P.C., et al., eds., Mesozoic and Cenozoic sequence stratigraphy of European basins: SEPM (Society for Sedimentary Geology) Special Publication 60, p. 75–80.

Bunker, B.J., Witzke, B.J., Watney, W.L., and Ludvigson, G.A., 1988, Phanerozoic history of the central Midcontinent, United States, *in* Sloss, L.L., ed., Sedimentary cover: North American craton, U.S.: Boulder, Colorado, Geological Society of America, Geology of North America, v. D-2, p. 243–260.

Burgess, P.M., Gurnis, M., and Moresi, L., 1997, Formation of sequences in the cratonic interior of North America by interaction between mantle, eustatic, and stratigraphic processes: Geological Society of America Bulletin, v. 109, p. 1515–1535.

Coogan, J.C., and Royse, F., Jr., 1990, Overview of recent developments in thrust belt interpretation, *in* Roberts, S., ed., Geologic field tours of western Wyoming and adjacent Idaho, Montana, and Utah: Geological Survey of Wyoming Public Information Circular 29, p. 89–124.

Cross, T.A., 1986, Tectonic controls of foreland basin subsidence and Laramide style deformation, western United States, *in* Allen, P., and Homewood, P., eds., Foreland basins: International Association of Sedimentologists Special Publication 8, p. 15–39.

DeCelles, P.G., 1994, Late Cretaceous–Paleocene synorogenic sedimentation and kinematic history of the Sevier thrust belt, northeast Utah and southwest Wyoming: Geological Society of America Bulletin, v. 106, p. 32–56.

Dyman, T.S., Merewether, E.A., Molenaar, C.M., Cobban, W.A., Obradovich, J.D., Weimer, R.J., and Bryant, W.A., 1994, Stratigraphic transects for Cretaceous rocks, Rocky Mountains and Great Plains regions, *in* Caputo, M.V., et al., eds., Mesozoic systems of the Rocky Mountain region, USA: Denver, Colorado, Rocky Mountain Section, SEPM (Society for Sedimentary Geology), p. 365–392.

Flemings, P.B., and Jordan, T.E., 1990, Stratigraphic modeling of foreland basins: Interpreting thrust deformation and lithosphere rheology: Geology, v. 18, p. 430–434.

Gill, J.R., and Cobban, W.A., 1973, Stratigraphy and geologic history of the Montana Group and equivalent rocks, Montana, Wyoming, and North and South Dakota: U.S. Geological Survey Professional Paper 776, 37 p.

Gurnis, M., 1992, Rapid continental subsidence following the initiation and evolution of subduction: Science, v. 255, p. 1556–1558.

Jordan, T.E., 1981, Thrust loads and foreland basin evolution, Cretaceous, western United States: American Association of Petroleum Geologists Bulletin, v. 65, p. 2506–2520.

Kauffman, E.G., Sageman, B.B., Kirkland, J.I., Elder, W.P., Harries, P.J., and Villamil, T., 1993, Molluscan biostratigraphy of the Cretaceous Western Interior basin, North America, *in* Caldwell, W.G.E., and Kauffman, E.G., eds., Evolution of the Western Interior basin: Geological Association of Canada Special Paper 39, p. 397–434.

Lithgow-Bertelloni, C., and Gurnis, M., 1997, Cenozoic subsidence and uplift of continents from time-varying dynamic topography: Geology, v. 25, p. 735–738.

Merewether, E.A., Blackmon, P.D., and Webb, J.C., 1984, The mid-Cretaceous Frontier Formation near the Moxa arch, southwestern Wyoming: U.S. Geological Survey Professional Paper 1290, 29 p.

Obradovich, J.D., 1993, A Cretaceous time scale, *in* Caldwell, W.G.E., and Kauffman, E.D., eds., Evolution of the Western Interior basin: Geological Association of Canada Special Paper 39, p. 379–396.

Pang, M., and Nummedal, D., 1995, Flexural subsidence and basement tectonics of the Cretaceous Western Interior basin, United States: Geology, v. 23, p. 173–176.

Royse, F., Jr., 1993, An overview of the geologic structure of the thrust belt in Wyoming, northern Utah, and eastern Idaho, *in* Snoke, A.W., et al., eds., Geology of Wyoming: Geological Survey of Wyoming Memoir 5, p. 273–311.

Yonkee, W.A., DeCelles, P.G., and Coogan, J.C., 1997, Kinematics and synorogenic sedimentation of the eastern frontal part of the Sevier orogenic wedge, northern Utah, *in* Link, P.K., and Kowallis, B.J., eds., Proterozoic to Recent stratigraphy, tectonics and volcanology, Utah, Nevada, Southern Idano, and central Mexico: Brigham Young University Geology Studies, v. 42, part 1, p. 355–380.



Manuscript received 8 November 2003
Revised manuscript received 28 January 2004
Manuscript accepted 30 January 2004

Printed in USA